

In Vitro Characterization of Electrodeposited Hydroxyapatite Coatings on Titanium (Ti6AL4V) and Magnesium (AZ31) Alloys for Biomedical Application

R.B. Durairaj¹, S. Ramachandran^{2,*}

¹ Research Scholar, School of Mechanical Sciences, Sathyabama Institute of Science and Technology, Chennai, India.

² Research Professor, School of Mechanical Sciences, Sathyabama Institute of Science and Technology, Chennai, India.

*E-mail: aishram2006@gmail.com

Received: 23 January 2018 / *Accepted:* 16 March 2018 / *Published:* 10 April 2018

Metallic implant, which is widely used in orthopedic and dental applications, should be removed once the healing process is completed. Removal of implants requires another surgery with psychological stress and economic burden. Biodegradable metallic implants have attracted researcher's attention as these implants are degraded and absorbed in the human body after the healing process is done. Among the various degradable metals, magnesium and its alloys are found to have similar physiochemical characteristics to that of natural bone. However, fast degradation and high corrosion rates limit its efficient use as implants. Coating over magnesium alloys can limit the degradation and corrosion rates so as to make implants of tailor-made performance. In this paper, chemically synthesized hydroxyapatite (HA) is coated over titanium (Ti6AL4V) and magnesium alloy (AZ31) substrates by electrodeposition technique. The coated and uncoated samples are subjected to electrochemical corrosion to examine the corrosive behavior of the coatings. The in vitro examination is undergone in simulated body fluid solution to identify the formation of bio growth of the HA coated Magnesium and Titanium alloy samples. SEM, EDS, FTIR analyses are used for characterization of the coatings. The results are obtained and discussed. The results show that the degradation and corrosion rates of HA coated Ti6AL4V and AZ31 are lower than that of uncoated samples. However, HA coated AZ31 seems to be a promising candidate for degradable implant applications as it supports bio-growth, while there is no significant bio-growth is observed in HA coated Ti6AL4V alloy.

Keywords: biomedical, hydroxyapatite, electro-deposition, magnesium, titanium, degradable implants, corrosion.

1. INTRODUCTION

While simple bone fractures can be treated by external fixation, bone fractures usually require internal fixation that uses implants (through surgery) to provide adequate temporary support at the fracture site for enhanced healing of the fracture. Metallic implants, made of stainless steels and titanium alloys, are the traditional materials used for internal fixations (in the form of plates, screws and pins) due to their high mechanical strength, high toughness, and high corrosion resistance. However, for patients of age below 40 years, implants should be removed after healing as they can cause stress shielding (mismatch of mechanical properties of implant material and human bone) and adverse physiological responses. In the case of children, removal of implants is compulsory so as to facilitate developmental bone growth. Removal of implants requires another surgery with psychological stress and economic burden. The use of traditional metallic implants sometimes creates a dilemma whether to remove the temporary implants and to retain permanently. The problem of traditional implants can be overcome by the use of degradable implants, which are subsequently absorbed in the human body [1,2]. Stainless steels, Cobalt alloys and titanium alloys are commonly used implant materials. However, these implants, such as plates, screws and pins, that are used to repair bone fractures, should be removed after the healing process is fulfilled. The removal of implants is generally done by a second surgery with associated risks. The use of degradable materials in such circumstance can provide benefit to avoid the need of second surgical procedure, cost or any associated health risks [3]. For example, titanium and its alloys are largely used as orthopedic and dental implants due to high corrosion resistance, high biocompatibility, high strength-to-weight ratio, and low elastic modulus. But, the elastic modulus of metallic implant is different from the surrounding bone tissues, and this mismatch possibly causes stress-shielding phenomena that impart stress at the bone-implant interface causing implant loosening, bone resorption and implant failures [4]. Metallic implants are also susceptible to bacterial infection. The local defense system is highly affected by the surgical trauma after implantation, and it is highly susceptible time for bacterial infection. The defense mechanism at the implant-tissue interface is affected even after tissue integration due to less number of blood vessels. The reduced defense mechanism causes colonization of bacteria resulting infection. Hence, the use of metallic implants leads to complications such as prolonged hospitalization, removal of implants, financial burden, implant failure, and even death. As a result, there is a need of preventive measures to put off the implant-induced bacterial infections, such as antibacterial coatings [5,6].

Biodegradable implants are regarded as superior to permanent implants in the biomedical applications. Permanent implants are non-degradable and remain even after the healing process is completed, which, in long term, may cause some troubles including sensitization, allergy, physical irritation and/or other physical problems. On the other hand, biodegradable implants are degraded and absorbed in the human body after healing. Biodegradable implants also reduce the overall cost as they do not require extra surgery for removal. Some of the most accessible degradable implants, obtained from polymers or ceramics, are poly-L-lactic acid, polyglycolic acid, polyglyconate and calcium phosphate ceramics. But, the polymeric materials show poor mechanical strength as compared to that of the metallic materials. Therefore, metallic biodegradable materials show high potential for biomedical implant applications due to their outstanding mechanical strength, biocompatibility and

non-toxicity [7,8]. Mg-based alloys, Fe-based alloys, and Zn-based alloys have been considered as efficient degradable metals for metallic implants. All three metals (iron, magnesium and zinc) are the essential nutritional substances for human body. However, the recommended intake of magnesium is about 240-420 mg/day, while it is 8-18 mg/day for iron (17-50 times lower than that of magnesium) and 8-11 mg/day for zinc (30-40 times lower than that of magnesium). Hence, pure zinc implants possibly raise a concern over the recommended daily intake and related health risks associated with high dosage of zinc. Magnesium-based alloys show significant advantages over ferrous alloys and zinc alloys. The elastic modulus of natural bone is about 3-20 GPa, while it is about 43 GPa, 211.4 GPa and 90 GPa for Magnesium, iron and zinc respectively. Elastic modulus of magnesium is very close to that of natural bone. The mismatch of elastic modulus in iron and zinc possibly will cause stress shielding. Both pure iron and pure magnesium are good candidates in terms of biocompatibility. However, iron accumulates and retains the corrosion products over 9 months which may prevent the tissue growth. On the other hand, magnesium implants are proven to stimulate the new bone formation from the time they are implanted. Therefore, research on magnesium and its alloys is vital for biodegradable implants [9,10,11].

Magnesium and its alloys are investigated for clinical use for the last two centuries by variety of surgeons (cardiovascular, musculoskeletal and general surgery). Magnesium is degradable and it dissolves completely in 9-10 months without any pain or infection. Most of the patients reported no pain or infection after magnesium implants, although they could feel subcutaneous foams or cavities due to fast implant corrosion. Even after two centuries, it is noticeable that Magnesium and its alloys are not yet commercially successful and much attention is required to advance further in the field of degradable metallic implants [12]. Magnesium is one of the light-weight metals which has the density of 1.74 g/cm^3 , this is very close to that of the natural bones ($1.8\text{--}2.1 \text{ g/cm}^3$). Magnesium's density is 1.6 and it is 4.5 times lesser as compared to aluminium and steel, respectively. Magnesium alloys are light weight, whose density is only one-third of that of titanium based alloys and one-fifth of that of stainless steel. The elastic modulus and compressive strength of magnesium are also comparable to that of cortical bone. However, magnesium and its alloys maintain the mechanical integrity over a period of 12–18 weeks. The unfortunate problem with pure magnesium is the high corrosion rate and fast degradation in the environment (pH of 7.4–7.6 and high chloride) which can cause losing of mechanical integrity of magnesium implants before the healing process is accomplished. Magnesium and its alloys suffer from attack of chloride containing environment, such as human body fluids or blood plasma [13,14]. Appropriate alloying or surface treatment provides sufficient strength requirement for efficient bone healing process. The simplest method to overcome the problems of fast degradation and high corrosion rate is coating rather than alloying, which provides a protective layer against the corrosive environment [15].

Hydroxyapatite ($\text{Ca}_{10}(\text{PO}_4)_6(\text{OH})_2$), that is basically pure calcium phosphate, has favorable osteo-conductive and bioactive properties making it a preferred biomaterial for both dental and orthopedic biomedical applications. The chemical composition and crystal structure of HA is very similar to apatite of the human skeletal system, which is therefore a more suitable material for bone substitution and reconstruction [16,17]. HA is one of the widely used coating materials in orthopedic and dental applications due to its superior biocompatibility and strong bonding with human bones. The

traditional HA coated bioceramics, however, show poor mechanical strength and promote bacterial growth which in turn may be the reasons for implant rejections. Addition of elements, has antibacterial properties, such as silver (Ag), zinc (Zn), copper (Cu), cerium (Ce), samarium (Sm), etc., may be beneficial to effectively prevent bacterial infections [2]. In the bone surgery, osseointegration is an important and desirable goal, and HA coated implants show high efficiency. However, the coating parameters such as location, composition, uniformity, thickness, etc. can influence the efficiency and robustness of HA coating [18]. There are mixed reports in favor or against HA coating on dental implants in terms of long-term survival of implants. In the work of Lee et al. [19], meta-analysis is performed to resolve the controversy on the reliability of HA coatings to dental implants. The survival rates of HA coated implants varied from 93.2% to 98.5%, for a period of 4 to 8 years of follow-up, while they varied from 79.2% to 98.5%, for the period of 5 to 8 years of follow-up. The survival rates remained above 90% and showed high reliability of HA coatings in dental implants. Similar work is done by Alfaiate et al. [20] and Herrera et al. [21], and concluded that the HA coated implants showed high survival rates compared to other implants.

HA coatings are evaluated on various substrates by research community. HA coating can be done using various coating techniques, such as plasma spraying, pulsed laser-deposition, sputtering, sol-gel, electro-deposition, electrophoresis etc. Among these techniques, electro-deposition of HA is regarded as an inexpensive and simple process that can be performed at a room temperature. The chemical composition and thickness of HA coating can easily be controlled by appropriately modifying the electro-deposition conditions. In the work of Song et al. [22], HA coating is performed on AZ91D magnesium alloy using electro-deposition method to improve the degradation in human body environment. The HA coating is found to delay the corrosion rate of magnesium alloys (10 times slower than the uncoated AZ91D) in stimulated body fluids and that could provide sufficient protection on magnesium alloys. In the work of Shi et al. [23], the composite coating of Ca-P is carried out by micro-arc oxidation followed by electrodeposition on AZ80 magnesium alloy. The effect of coating on corrosion rate and apatite-formability in simulated body fluids are investigated and the results show that the composite coating significantly reduce the corrosion rate and enhance apatite-formability of magnesium alloy. The corrosion resistance of HA coating on porous magnesium is investigated by Kang et al. [24]. HA coating is performed by immersing the porous magnesium in the aqueous solution (of ethylenediaminetetraacetic acid calcium disodium salt hydrate and potassium phosphate monobasic in distilled water) for 6 h. The compressive strength increases remarkably from 8 MPa to 17 MPa. It is also found that bio-corrosion of the porous magnesium is inhibited significantly by HA coating. Plasma spraying process is commonly used for HA coatings for fixing implants due to extreme high temperatures. However, they unfortunately degrade easily in a short time after implantation, which may reduce the adhesion of HA layer. In the work of Stoch et al. [25], electrophoretic deposition was successfully used for preparing the HA coating on titanium implants and found that the process do not change the properties of HA coatings as compared to the pure HA powder. Kim et al. [26] investigated the HA coating over Magnesium in an aqueous solution of calcium and phosphate and found that HA coating remarkably reduced the corrosion rate in a simulated body fluid. From the literatures, it is noticed that HA coating reduced the corrosion rates.

The purpose of this article is to evaluate the applicability of HA coating on two different implant metals (magnesium and titanium alloys) of which one is degradable and the other is non-degradable. HA is synthesized from calcium and phosphorus, and the coated implants are prepared over titanium alloy (Ti6AL4V) and magnesium alloy (AZ31) substrate materials using electrodeposition. After conditioning, corrosion experiments are performed for the coated samples using electrochemical corrosion. The bio-growth is also observed in immersion of the samples in the simulated body fluid. The morphological changes of the surfaces are observed in SEM, EDS and FTIR analyses. The results are obtained and discussed.

2. EXPERIMENTAL PROCEDURE

2.1. Substrate materials

Two commercially available surgical grade substrates are purchased from local market near Park Town, Chennai. Two alloys of titanium alloy of grade Ti6AL4V and magnesium alloy of grade AZ31 are used as the substrate materials. The chemical compositions of the materials are shown in the table 1. The substrates are cut into pieces of square shapes with a side of 1 cm. The surface of the pieces is treated with silicon carbide emery sheet followed by ultrasonic rinsing with distilled water before the start of coating process.

Table 1. Chemical Composition of Substrate Materials

S. No.	Material	Composition
1	Titanium Alloy (Ti6AL4V)	Titanium 98.605, Carbon 0.8, Oxygen 0.25, Nitrogen 0.030, Iron 0.30 and Hydrogen 0.015
2	Magnesium Alloy (AZ31)	Magnesium 96.42, Manganese 0.321, Iron 0.0030, Copper 0.0010, Nickel 0.0020, Titanium 0.0100, Aluminum 2.51 , Zinc 0.7200

2.2. Hydroxyapatite Synthesis

Hydroxyapatite is the coating material which is synthesized from calcium nitrate and diammonium hydrogen phosphate in the laboratory at International Research Centre, Sathyabama University, Chennai. 0.4 M of calcium nitrate and 0.239 M of diammonium hydrogen phosphate are taken in separate beakers. 500 ml of distilled water is added to each beaker separately and stirred continuously at 350 rpm to make aqueous solutions. The calcium nitrate and diammonium hydrogen phosphate solutions are then transferred to another beaker where the diammonium hydrogen phosphate solution is added slowly at a flow rate of 3ml/min until pH is maintained at 7. It is observed that the color of the solution changes to milky white (hydroxyapatite). The solution is aged overnight and dried. It is then conditioned in an oven at 80°C to and crushed into powder.

2.3. Electrodeposition of Hydroxyapatite

HA coatings are performed using electrodeposition method. The electrodeposition is performed in the set-up shown in figure 2. It consists mainly of voltage regulator with a magnetic stirrer. Electrodeposition is carried out in a beaker of electrolytic solution. HA powder solution acts as the electrolytic solution. Ti6AL4V and AZ31 act as the working electrode (cathode) and platinum (anode) as reference electrodes. Electrodeposition is carried out at constant voltage and current of 5V and 5 mA respectively at room a temperature for 2 h. By adjusting voltage regulator, the voltage and current can be adjusted. The coated materials are removed from the set-up and the process is repeated for all specimens. The coating thickness is measured at various locations using a micrometer to ensure the coating uniformity over the substrate surfaces.

2.4. Simulated body fluid (SBF)

Simulated body fluid (SBF), which is identical to human blood plasma, is used for simulating the bio-activity of the bone-bonding bioactivity for bioactive materials, titanium and magnesium alloys. This solution is prepared by standard procedure (with composition of NaCl 7.996, KCl 0.224, CaCl₂.2H₂O 0.278; MgCl₂.6H₂O 0.305; NaHCO₃ 0.350; K₂HPO₄.3H₂O 0.228; Na₂SO₄ 0.071). The SBF solution is prepared for the development of bio-growth on the coated surface by soaking the samples of HAP coated Ti6AL4V and AZ31 substrates. The ionic concentrations of SBF solution are tabulated as shown in Table 2. The ion concentrations of SBF are close to that of human blood plasma and can therefore effectively be simulated for bio-growth.

Table 2. Ionic Concentration of SBF and Human Blood Plasma

	Na ⁺	K ⁺	Mg ²⁺	Ca ²⁺	Cl ⁻	HCO ₃ ⁻	HPO ₄ ²⁻	SO ₄ ²⁻
Blood plasma	142.0	3.6-5.5	1.0	2.1-2.6	95.0-107.0	27.0	0.65-1.45	0.5
SBF	142.0	6.5	1.5	2.5	18.0	4.2	1.0	0.4

2.5. Electrochemical Corrosion

Electrochemical corrosion rates are determined with the help of potentiodynamic polarization technique at International Research Centre, Sathyabama University, Chennai. In this examination, there are three electrodes, (platinum as counter electrode; HA coated Ti6AL4V and AZ31 as the working electrodes and saturated calomel electrode as the reference electrode) used in a polarization cell. SBF solution (100 ml) is used as the electrolyte solution. Each square shaped sample (working electrodes) of size of 1cm X 1cm is attached to a holder. The temperature of 38°C is maintained (which is similar to that of a human body). The electrodes are attached to potentiostat which is utilized to control the potential for controlling the polarization scan rate. The scan rate of 0.1667 mV/s is used in the experiment. An electrochemical potential is produced between the various electrodes with the

help of the potentiostat, and the corrosion potential (E_{CORR}) and the corrosion current (I_{CORR}) are recorded. The corrosion rates are then calculated.

2.6. Bio-growth in SBF

The in vitro examination of the HA coated substrates is conducted by immersing the coated samples (1cm X 1cm) in SBF solution over a period of 0-7 days. The samples of HA coated Ti6AL4V and AZ31 are soaked separately in the SBF solution, which is replaced by fresh SBF solution for every 48 hours. After this period, the samples are washed clearly and conditioned in the oven at 80°C for 30 minutes. The formation of bio-growth over the sample surfaces are observed in SEM.

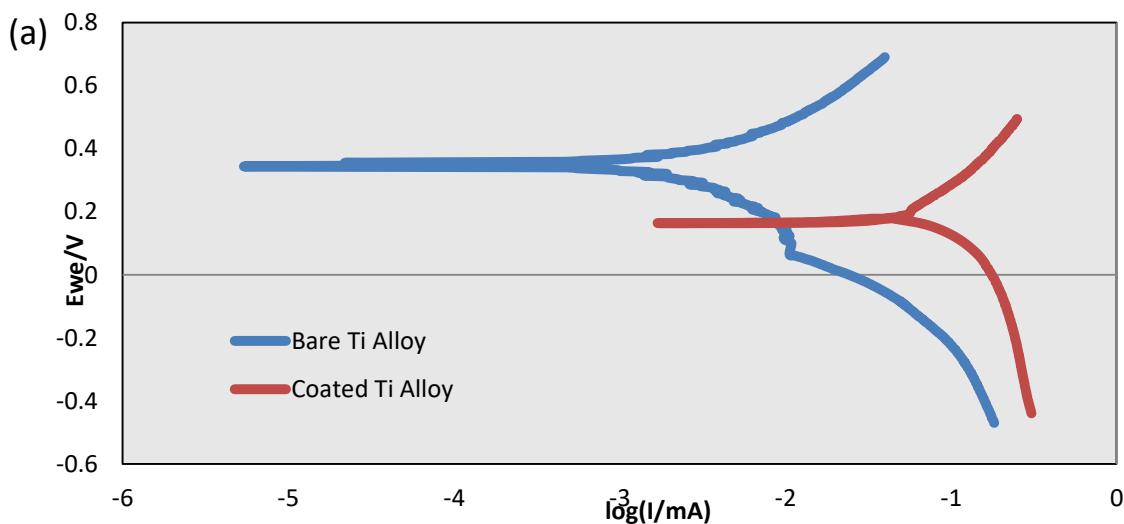
2.7. Surface Morphology

The surface morphological behavior of the coated samples is observed through an SEM equipment of CARL ZEISS AG brand (International Research Centre, Sathyabama University, Chennai). The observations are made on the coated samples before and after in vitro examination. In addition, Fourier Transform-Infrared Spectroscopy (FTIR) analysis (Thermo Fisher Scientific at FIST lab of Sathyabama University, Chennai) and Energy Dispersive X-Ray Spectroscopy (EDS) analysis (Sathyabama University, Chennai), at Intertek Wilton equipment, are also carried out for certain surface morphology.

3. RESULTS AND DISCUSSION

3.1. Electrochemical Corrosion

The potentiodynamic polarization curves of the HAP coated AZ31 and Ti6AL4V substrates are obtained from the SBF solution as shown in Figure 1 (a) and (b).



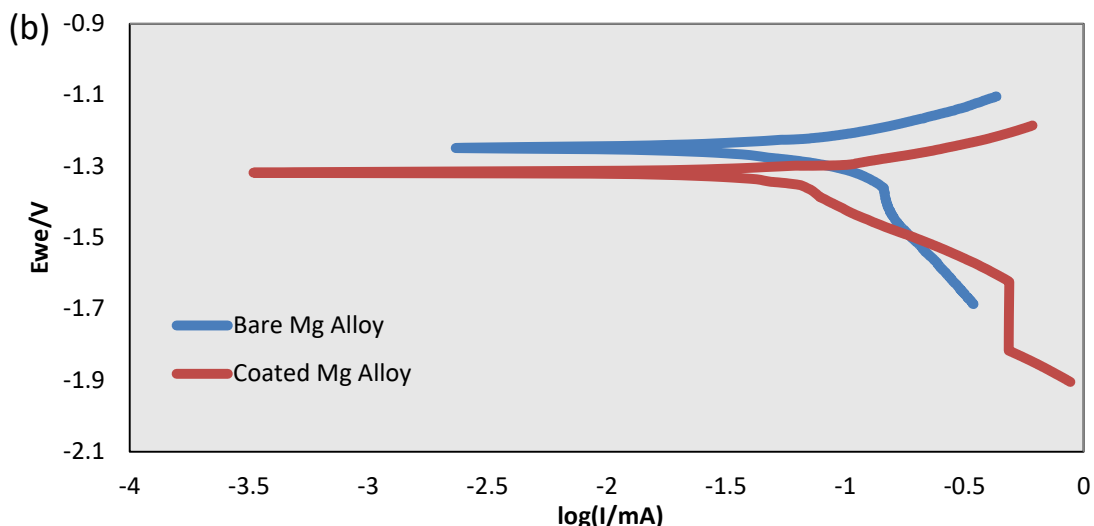


Figure 1. Electrochemical Corrosion Plot of (a) HA Coated Ti6AL4V (b) HA coated AZ31

Table 3. E_{CORR} , I_{CORR} and Corrosion Rates of the HA Coatings

S. No.	Sample	E_{CORR} (mV)	I_{CORR} (μ A)	Corrosion Rate (mm/year)
1	AZ31 (Uncoated)	-1252.23	97.31	2.703
2	AZ31 (Coated)	-1337.07	53.20	1.477
3	Ti6AL4V (Uncoated)	216.25	85.05	0.962
4	Ti6AL4V (Coated)	337.67	2.24	0.062

The corrosion potential (E_{CORR}) and the current density (I_{CORR}) values of the HAP coated substrates are obtained for the polarization curves and presented in Table 3.

The polarization curve (corrosion graph) is obtained between Log (I/mA) and Ewe/v for both uncoated and HA coated samples. It records the association between the applied potential and the current density. The coated substrates exhibit higher current densities than that of the uncoated substrates. The degradation of coated materials is considered to be lesser than that of uncoated materials. Therefore, the corrosion resistance of the HA coated samples are improved on all the samples. Corrosion rates are settled on using Tafel equation and the average values of the test samples are tabulated in the table 3. The corrosion rate of HA coated AZ31 is 1.477 mm/year, while the same of the uncoated AZ31 substrate is 2.703 mm/year. In case of HA coated Ti6AL4V substrate, the corrosion rate is very less (0.062 mm/year), when compared to uncoated substrate (2.362 mm/year). In the curve (figure 4), one can observe that the disconnected lines which are due to the presence of porous regions in the coatings. It is also noted that both HA coated magnesium and titanium alloys show the delayed corrosion of the base material and better resistance to corrosion as compared to that of uncoated substrates.

3.2. In Vitro test

The in vitro Examination of HA coated AZ31 and Ti6AL4V substrates are shown in Figure 5. The apatite formation is recognized with the white colour regions in the SEM images [39]. The observations of AZ31 samples are made on 3rd and 7th days after immersing the substrates in SBF solution and the SEM images are presented in the figure 2 (a) and (b).

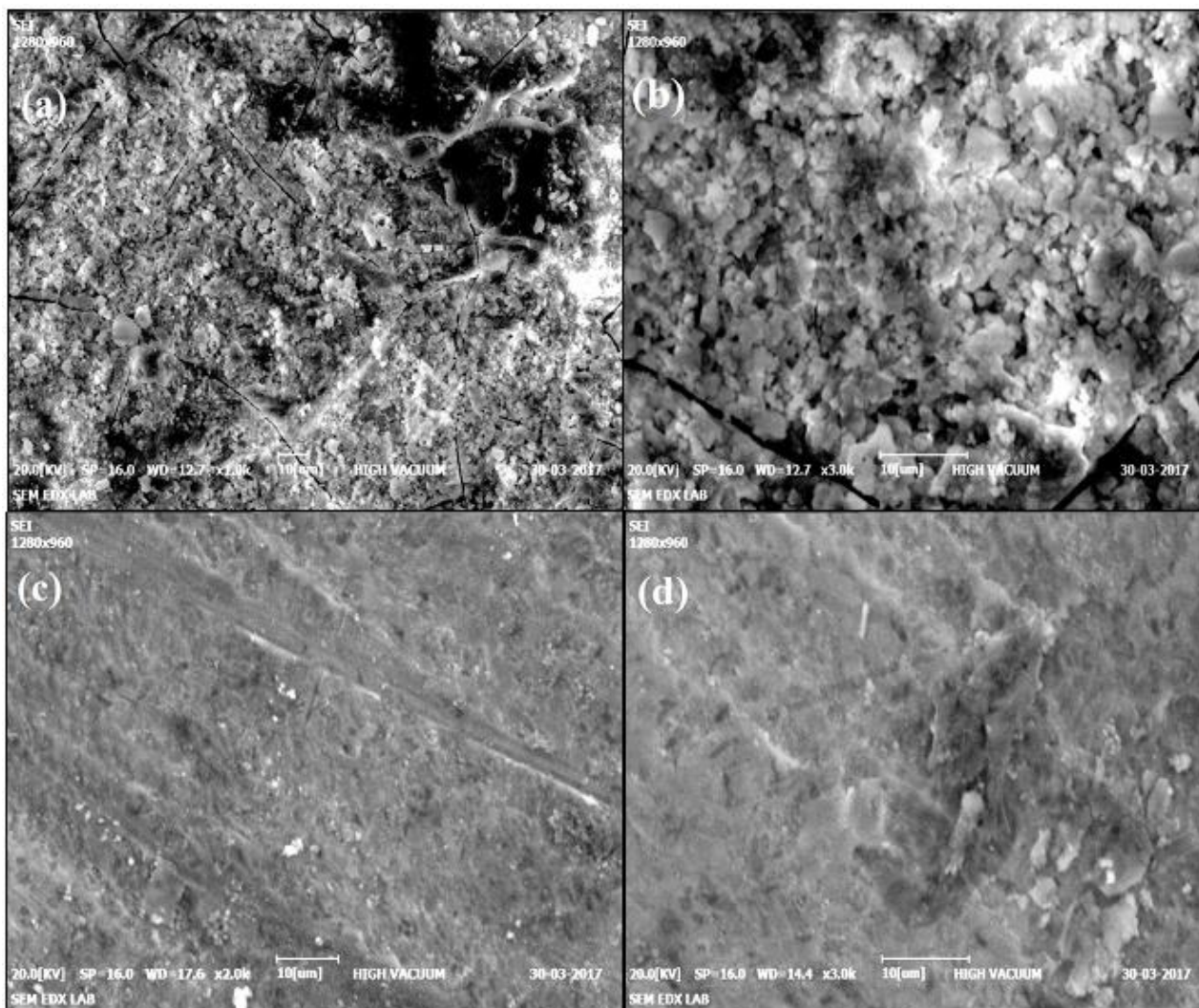


Figure 2. SEM images representing bio growth of HA coated samples soaked in SBF (a) AZ31 for 3 days (b) AZ31 for 7 days (c) Ti6AL4V for 3 days (d) Ti6AL4V for 7 days.

It is observed that the formation of apatite (white colored layer) over the surface of AZ31 is less found in 3rd day image, but remarkable change is found in the 7th day image. In the 7th day image, the tissue growth is spotted in three to four regions. This showcases that HA coating advanced biogrowth and is regard as biocompatible with the human tissues. On the other hand, in the case of Ti6AL4V substrate, a very thin and small layer of the apatite formation is observed as compared to that of AZ31, as shown in the figures 2 (c) and (d). No significant change is noticed on the 3rd day

image, and small spots of apatite layer are noticed on the 7th day image. The biocompatibility of HA coated Ti6AL4V alloy is lesser than that of magnesium alloy. However, the results project that the apatite formation of HA coated AZ31 samples are greater than that of uncoated Ti6AL4V samples. The results also show that the biocompatibility of AZ31 is promising, as opposed to Ti6AL4V which does not support bio-growth immediately and remained as the foreign material in the human body.

3.3. Surface morphology of the Substrates

The SEM images are taken for the HA coated AZ31 (figure 3a & b) and Ti6AL4V (Figure 3 c&d) substrates. In Figure 3(a) & (b), it is observed that the formation of flower-like structures is observed in the AZ31 alloy, which is similar to the ones reported in [27, 28]. The white colour distributed over the flower-like structure is due to the presence of HA coating.

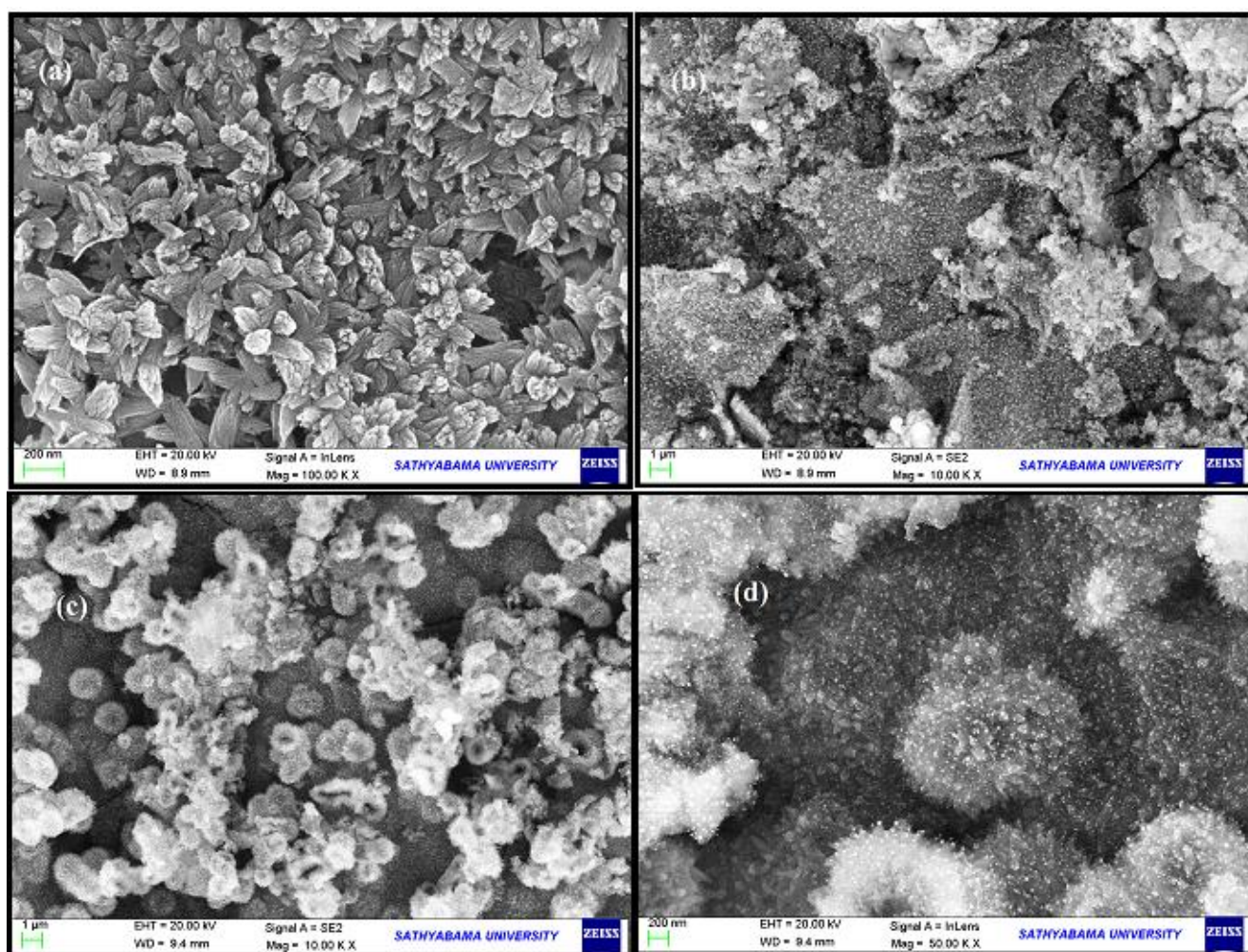


Figure 3. SEM Images of (a) uncoated AZ31, (b) HA coated AZ31, (c) uncoated Ti6AL4V, (d) HA coated Ti6AL4V

This HA deposition underwent crystalline formation and occupied the entire surface of the AZ31. In Figure 3 (c) & (d), the deposition of HA over the surfaces of Ti6AL4V alloy is shown, which is similar to the SEM image of Xia et al. [33]. The HA coated Ti6AL4V surface showed the formation of ball-like structure with small white spots of HA crystal is observed on the surface.

3.4. Fourier Infrared Spectra

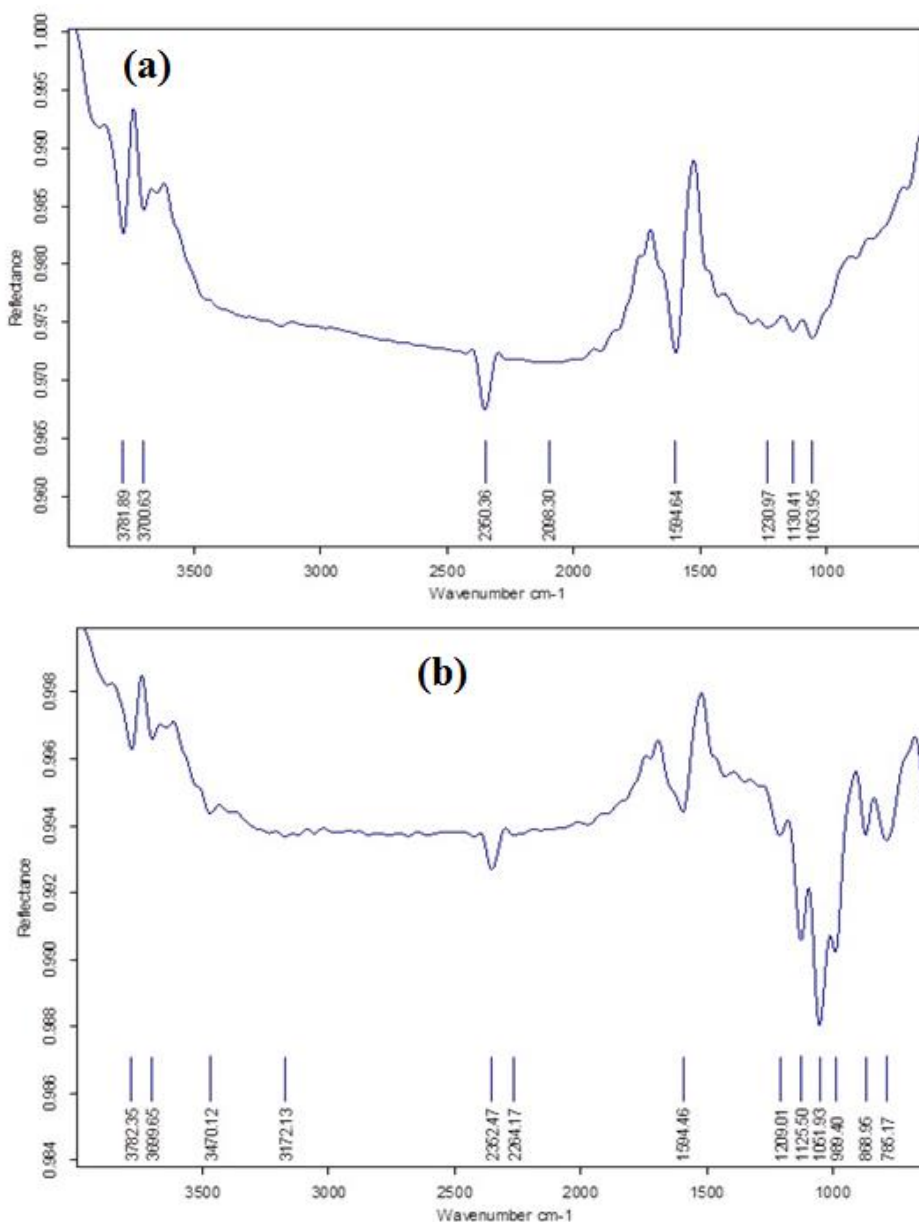


Figure 4. FTIR Spectra of HA coated samples for (a) AZ31 (b) Ti6AL4V

The FTIR pattern is obtained for the HA coated AZ31 (Figure 4a) and Ti6AL4V (Figure 4b) substrates. In the FTIR image of AZ31, it is observed that the wave numbers ranged from 1200 to 1300 cm^{-1} with range of 0.992 to 0.993 reflectance for the AZ31 substrate. Also a double peak is identified in wave numbers 1200 to 1100 cm^{-1} which is similar to the double peak observed. It is also observed some of the smaller peaks in 900 – 700 cm^{-1} of the AZ31 substrates these peaks shows the presence of

HA over the substrate surface. Similarly for the Ti6AL4V substrates, the huge peak is noted at 1500 cm^{-1} of wave numbers, a small double peak is observed at 1700 cm^{-1} and a depth is formed at $900 - 1000\text{ cm}^{-1}$. This may be due to the improper deposition of the HA over the Substrate surface.

3.5. Energy dispersive spectra

The EDS spectra of HA coatings are obtained for AZ31 (figure 5 a) and Ti6AL4V (figure 5 b). For AZ31, the elements found are Ca, P, O and Mg and this is similar to the prior literature [30, 31]. It is observed that 8–9 % of Ca and 2–5 % of P, 23 % of oxygen and 78% of Mg are also found in this EDS spectra. In Figure 5 (b), the elements and allocation of the elements are presented for HA coated Ti6AL4V alloy. The elemental proportions are similar to the ones acknowledged by other literatures [31, 34, 35]. The presence of Ti 35%, Na 1%, Cl 1% and oxygen 45% are also evidenced on the coated surface of the Ti6AL4V. The standard percentage of Ca is 18% and P is 10%. This shows that the presence of HA helps in biogrowth of the substrate.

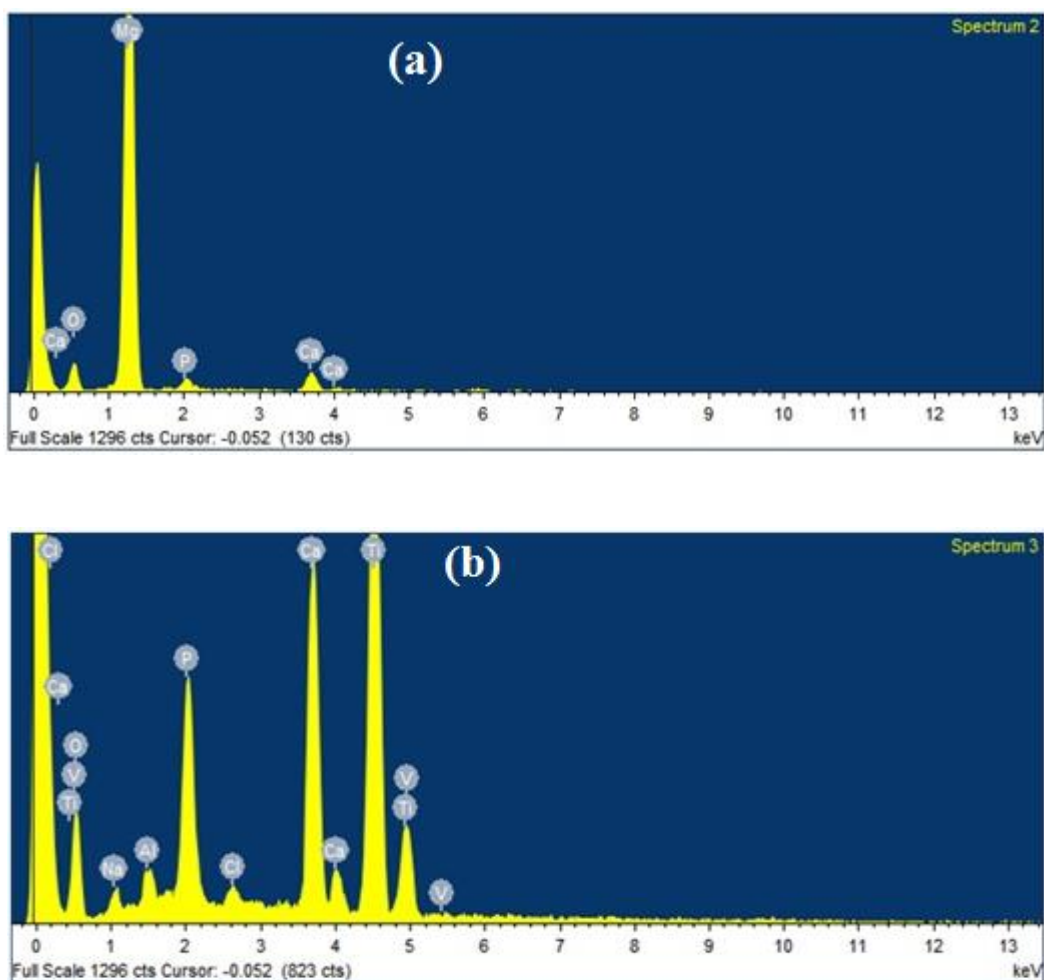


Figure 5. (a) EDS images of HA Coated (a) AZ31 (b) Ti6AL4V

4. CONCLUSION

In this work, the effects of HA coating over AZ31 and Ti6AL4V substrates on corrosion rate and bio-growth are presented and discussed. The coating is carried out by electrodeposition method. The samples are prepared and subjected to various experiments. The results are obtained and discussed in the previous sections. The conclusion of the research is summarized as follows: The HA coatings are formed a protective layer over the AZ31 and Ti6AL4V substrates and achieved the corrosion of 1.477 mm/year and 0.062 mm/year respectively. The immersion examination revealed that the formation of apatite layer of HA coated AZ31 is greater due to the presence of larger regions of apatite, while HA coated Ti6AL4V shows only minor spots. From the results, it is concluded that HA coated magnesium alloy AZ31 seems to be good candidate for degradable implant applications with reduced corrosion and degradation rates. The results open ways to prepare tailor-made corrosion and degradation rates as per the requirements of healing time. Further, investigation is required to determine the effects of coating thickness and composition of magnesium alloys over degradation rates to meet the requirements of tailor-made implants.

ACKNOWLEDGEMENT

Our sincere thanks to Mr. Gopi Saravanan, of International Research Center, Sathyabama University, Chennai, for providing constant support in conducting experiments for this research work.

References

1. K.Y. Chiu, M.H. Wong, F.T. Cheng and H.C. Man, *Surface & Coatings Technology*, 202 (2007) 590–598.
2. S. Sathishkumar, K. Louis, E. Shinyjoy, and D. Gopi, *Ind. Eng. Chem. Res.*, 55 (2016) 6331–6344.
3. Y. Xin, T. Hu and P.K. Chu, *Acta Biomaterialia*, 7 (2011) 1452–1459.
4. H. Huang, P.H. Lan, Y.Q. Zhang, X.K. Li, X. Zhang, C.F. Yuan, X.B. Zheng and Z. Guo, *Surface & Coatings Technology*, 283 (2015) 80–88.
5. L. Zhao, P.K. Chu, Y. Zhang and Z. Wu, *J. Biomedical Materials Research Part B: Applied Biomaterials*, 91B (2009) 470-480.
6. B. Kasemo, *The Journal of Prosthetic Dentistry*, 49 (1983) 832-837.
7. H.R. Bakhsheshi-Rad, E. Hamzah, M. Daroonparvar, R. Ebrahimi-Kahrizsangi and M. Medraj, *Ceramics International*, 40 (2014) 7971–7982.
8. Y. Yun, Z. Dong, N. Lee, Y. Liu, D. Xue, X. Guo, J. Kuhlmann, A. Doepke, H.B. Halsall, W. Heineman, S. Sundaramurthy, M.J. Schulz, Z. Yin, V. Shanov, D. Hurd, P. Nagy, W. Li, and C. Fox, *Materials Today*, 12 (2009) 22-32.
9. Y. Chen, Z. Xu, C. Smith and J. Sankar, *Acta Biomaterialia*, (2014) doi: <http://dx.doi.org/10.1016/j.actbio.2014.07.005>
10. Y.F. Zheng, X.N. Gu and F. Witte, *Materials Science and Engineering*, R77 (2014) 1–34.
11. H. Li, Y. Zheng and L. Qin, *Progress in Natural Science: Materials International*, 24 (2014) 414–422.
12. F. Witte, *Acta Biomaterialia*, 23 (2015) S28–S40.
13. M.P. Staiger, A.M. Pietak, J. Huadmai and G. Dias, *Biomaterials*, 27 (2006) 1728–1734.
14. C.K. Seal, K. Vince and M.A. Hodgson, *IOP Conf. Series: Materials Science and Engineering*, 4 (2009) 012011, 4 Pages.

15. Y. Shi, M. Qi, Y. Chen and P. Shi, *Materials Letters*, 65 (2011) 2201–2204.
16. E. Mohseni, E. Zalnezhad and A.R. Bushroa, *Int. J. Adhesion & Adhesives*, 48 (2014) 238–257.
17. S. Vahabzadeh, M. Roy, A. Bandyopadhyay and S. Bose, *Acta Biomaterialia*, (2015) 9 Pages.
18. S.B. Goodman, Z. Yao., M. Keeney and F. Yang, *Biomaterials*, 34 (2013) 3174–3183.
19. J.J. Lee, L. Rouhfar and O.R. Beirne, *J. Oral Maxillofac Surg*, 58 (2000) 1372–1379.
20. D. Alfaiate, T. Escobar, P. Oliveira, I. Almeida, D. Rosas and B. Borges, *Clin. Oral Impl. Res.*, 25 (Suppl. 10) (2014) 511–511.
21. A. Herrera, J. Mateo, J. Gil-Albarova, A. Lobo-Escolar, E. Ibarz, S. Gabarre, Y. Más and L. Gracia, *BioMed Research International*, Article ID 386461 (2015) 13 pages.
22. Y.W. Song, D.Y. Shan and E.H. Han, *Materials Letters*, 62 (2008) 3276–3279.
23. Y. Shi, M. Qi, Y. Chen and P. Shi, *Materials Letters*, 65 (2011) 2201–2204.
24. M.H. Kang, H.D. Jung, S.W. Kim, S.M. Lee, H.E. Kim, Y. Estrin and Y.H. Koh, *Materials Letters*, 108 (2013) 122–124.
25. A. Stoch, A. Brozek, G. Kmitha, J. Stoch, W. Jastrzebski and A. Rakowska, *J. Molecular Structure*, 596 (2001) 191–200.
26. S.M. Kim, J.H. Jo, S.M. Lee, M.H. Kang, H.E. Kim, Y. Estrin, J.H. Lee, J.W. Lee and Y.H. Koh, *J. Biomedical Materials Research A*, (2013) 1–13.
27. C. Wen, S. Guan, L. Peng, C. Ren, X. Wang and Z. Hu, *Applied Surface Science*, 255 (2009) 6433–6438.
28. S. Shadanbaz and G.J. Dias, *Acta Biomaterialia*, 8 (2012) 20–30.
29. Z. Shi, M. Liu and A. Atrens, *Corrosion Science*, 52 (2010) 579–588.
30. L. Xu, F. Pan, G. Yu, L. Yang, E. Zhang and K. Yang, *Biomaterials*, 30 (2009) 1512–1523.
31. M. Jamesh, S. Kumar and T.S.N.S. Narayanan, *J. Coat. Technol. Res.*, 9 (2012) 495–502.
32. A.L. Oliveira, R.L. Reis and P. Li, *J. Biomedical Materials Res Part B: Applied Biomaterials*, (2007) 258–265.
33. Z. Xia, X. Yu and M. Wei, *J Biomed Mater Res Part B*, 100B (2012) 871–881.
34. I.J. Hwang, H.C. Choe and W.A. Brantley, *Surface & Coatings Technology*, 320 (2017) 458–466.
35. H. Zhou, S. Kong, Y. Pan, Z. Zhang, L. Deng, *Materials Science and Engineering*, C56 (2015) 174–180.
36. F. Zhang, S. Cai, G. Xu, F. Wang, N. Yu, R. Ling, X. Wu, *Ceramics International*, 42 (2016) 18466–18473.
37. S. Shen, S. Cai, Y. Li, R. Ling, F. Zhang, G. Xu and F. Wang, *Chemical Engineering Journal*, 309 (2017) 278–287.
38. B. Zhu, Y. Xu, J. Sun, L. Yang, C. Guo, J. Liang and B. Cao, *Metals*, 7 (2017) 214, 12 Pages.
39. A.C.W. Noorakma, H. Zuhailawati, V. Aishvarya, and B.K. Dhindaw, *J. Materials Engineering and Performance*, (2013) DOI: 10.1007/s11665-013-0589-9.